Lattice Boltzmann approach for complex nonequilibrium flows

A. Montessori,[1,*] P. Prestininzi,[1] M. La Rocca,[1] and S. Succi[2]
[1]*Department of Engineering, University of Rome, "Roma Tre" Via Vito Volterra 62, 00146 Rome, Italy*
[2]*Istituto per le Applicazioni del Calcolo, CNR Via dei Taurini 19, 00185 Rome, Italy*
(Received 11 March 2015; published 22 October 2015; corrected 20 November 2015)

We present a lattice Boltzmann realization of Grad's extended hydrodynamic approach to nonequilibrium flows. This is achieved by using higher-order isotropic lattices coupled with a higher-order regularization procedure. The method is assessed for flow across parallel plates and three-dimensional flows in porous media, showing excellent agreement of the mass flow with analytical and numerical solutions of the Boltzmann equation across the full range of Knudsen numbers, from the hydrodynamic regime to ballistic motion.

DOI: 10.1103/PhysRevE.92.043308 PACS number(s): 47.11.−j, 47.45.Ab, 47.56.+r

I. INTRODUCTION

A deeper understanding of the physics of fluids at the microscale and nanoscale is key to many emergent applications in science and micronanoengineering [1–3]. Due to the inherent multiscale nature of the problem, with details at the nanometric scales affecting the overall operation of macroscopic devices, a whole array of computational techniques must be deployed to develop a quantitative understanding of these phenomena. As a result, in the last decades, several *mesoscale* methods have emerged in the attempt to bridge the gap between the macrolevels and microlevels [4–9]. Among others, the lattice Boltzmann (LB) approach appears to offer a very effective means of dealing with flow problems which are "too small" for the continuum mechanics and "too large" for molecular methods [10].

The Boltzmann equation is known to converge to the Navier-Stokes equations in the limit of vanishing Knudsen number, through the Chapman-Enskog asymptotic expansion. The same is true for the LB equation.

At finite-Knudsen numbers, higher-order generalized hydrodynamic equations, known as Burnett and super-Burnett, are obtained. However, the practical use of these equations has met with limited success, due to unstable behavior and other difficulties connected with the implementation of boundary conditions. It has been argued that the LB approach cannot deliver any reliable information in this finite-Knudsen generalized hydrodynamic regime, since it does not feature enough symmetry to recover the required high-order terms. However, numerous simulations have proved such theoretical expectations too restrictive and shown that the LB approach continues to provide useful information also beyond the hydrodynamic regime, where nonequilibrium effects can no longer be treated as a weak departure from local equilibrium. [11–13].

Subsequent developments have identified the main features that have to be added on top of the standard LB scheme in order to make it eligible for generalized hydrodynamic investigations, namely, (i) higher-order lattices (HOLs) [14–17], (ii) kinetic boundary conditions (KBCs) [18], and (iii) regularization (REG) [19,20]. KBCs are required to properly describe the momentum exchanges between fluid molecules and solid walls, so as to allow relative motion of the fluid in the near-wall region (slip motion). They stand in marked contrast with the no-slip boundary conditions used in continuum hydrodynamics which are typically implemented by the so-called bounce-back (BB) rule, i.e., particles impinging on the wall are bounced back along the opposite direction [15,18]. HOLs are necessary to provide sufficient isotropy for the description of the high-order kinetic moments carrying the relevant generalized hydrodynamic information. By HOLs we refer to those lattices which provide isotropy beyond the fourth order. Typical HOLs used in LB theory contain more kinetic moments than needed for hydrodynamic purposes, the so-called "ghosts," hence suitable filtering of such modes is a crucial step in the procedure. Finally, regularization filters out the nonhydrodynamic modes generated by the free motion of the molecules between two subsequent collisions, with the result of smoothing the effects of ghost modes [20–22]. The combination of the three features above, which we shall dub "extended LB" for brevity, bears a major conceptual and practical value, as it potentially leads to the accomplishment of the Grad's extended hydrodynamics approach [23] within a very compact and efficient computational framework [24]. It is clear that the successful completion of this program would lead to a significant gain (one or two orders of magnitude) in computational efficiency for Kn $\sim$ 1 flows. However, to date, a consolidated picture of how the above features combine to form a unified lattice kinetic approach capable of handling strong nonequilibrium effects across a broad range of Knudsen numbers is lacking.

In this paper, we show that all three ingredients are indeed necessary to correctly reproduce nonequilibrium behavior across the full range of Knudsen numbers, for the case of flow across flat parallel plates. On the other hand, we also show that for more complex geometries, such as three-dimensional flows through a regular array of spheres, global observables, say, mass flow, can be computed even by using simple bounce-back boundary conditions. Since such conditions are manifestly locally incorrect at finite-Knudsen numbers, the message is that the errors they introduce are alleviated by the regularization procedure, at least in a global sense, i.e., upon averaging over the entire fluid configuration. This may offer a handy shortcut for computational studies of nonequilibrium flows through disordered media.

*and.montessori@gmail.com

II. REGULARIZED LATTICE BOLTZMANN METHOD AND KINETIC BOUNDARY CONDITIONS

The lattice Boltzmann method is based on a minimal (lattice) version of the Bhatnagar-Gross-Krook equation, in which the computational molecules stream along the links of a uniform lattice, and collide on the nodes according to a simple relaxation to a local equilibrium. In equations,

$$f_i(\vec{x}+\vec{c}_i\Delta t,t+\Delta t) = f_i(\vec{x},t) + \frac{\Delta t}{\tau}\left[f_i^{\rm eq} - f_i(\vec{x},t)\right] + \frac{\Delta t}{c_s^2}\vec{c}_i\cdot\vec{F}, \quad (1)$$

where $f_i(\vec{x},t)$ is the discrete distribution function, representing the probability of finding a particle at position $\vec{x}$ and time t with discrete velocity $\vec{c}_i$, being i the index spanning over the lattice discrete directions, $i=0,\ldots,b$, [25]. Finally, Δt is the lattice time step. The left hand side of Eq. (1) represents the free-streaming of particles within the lattice, which hop from a lattice node to neighboring ones according to the direction defined by the lattice vector $\vec{c}_i$. The right hand side includes the forcing term and the collisional relaxation of the set of distribution functions towards the discrete local equilibria $f_i^{\rm eq}$, i.e., truncated low-Mach number expansion of the Maxwell-Boltzmann distribution. When using HOLs, the forcing term as in Eq. (1) should be modified to include a discrete correction [14]. However, we have verified that the results obtained are not affected by the type of forcing scheme. Indeed, by simulating the same flow with both flow boundary conditions (without a forcing term) and with a different kind of forcing scheme, namely, the exact difference method [26], we have obtained basically the same results. It is worth noting that while the low-order isotropic lattices are implemented with second-order equilibria, the high-order lattices are equipped with equilibria including kinetic moments up to third order. The second-order and third-order expansion of the Maxwell-Boltzmann distribution function used in this work reads as follows:

$$f_i^{\rm eq} = w_i\rho\left[1+\frac{(\vec{c}_i\cdot\vec{u})}{c_s^2}+\frac{(\vec{c}_i\cdot\vec{u})^2}{2c_s^4}-\frac{\vec{u}\cdot\vec{u}}{2c_s^2}\right], \quad (2)$$

$$f_i^{\rm eq} = w_i\rho\left[1+\frac{(\vec{c}_i\cdot\vec{u})}{c_s^2}+\frac{(\vec{c}_i\cdot\vec{u})^2}{2c_s^4}-\frac{\vec{u}\cdot\vec{u}}{2c_s^2} + \frac{(\vec{c}_i\cdot\vec{u})^3}{6c_s^6}-\frac{\vec{u}\cdot\vec{u}}{2c_s^4}(\vec{c}_i\cdot\vec{u})\right], \quad (3)$$

where w_i are weights of the discrete equilibrium distribution functions, c_s is the lattice sound speed, and $\vec{u}$ is the macroscopic flow velocity. The parameter τ in Eq. (1) is the relaxation time which controls the lattice kinematic fluid viscosity through the relation [25] $\nu = c_s^2(\tau - \frac{\Delta t}{2})$. We wish to point out that the use of third-order equilibria is motivated by the fact that the regularization procedure employed encompasses moments up to order three. As a result, the use of equilibria higher than third order would require an adaptation of the regularization step as well. Such an adaptation is conceptually straightforward, but it implies a significant computational overhead due to the need for computing the 15 components of the fourth-order tensor $\sum_i f_i\vec{c}_i\vec{c}_i\vec{c}_i\vec{c}_i$.

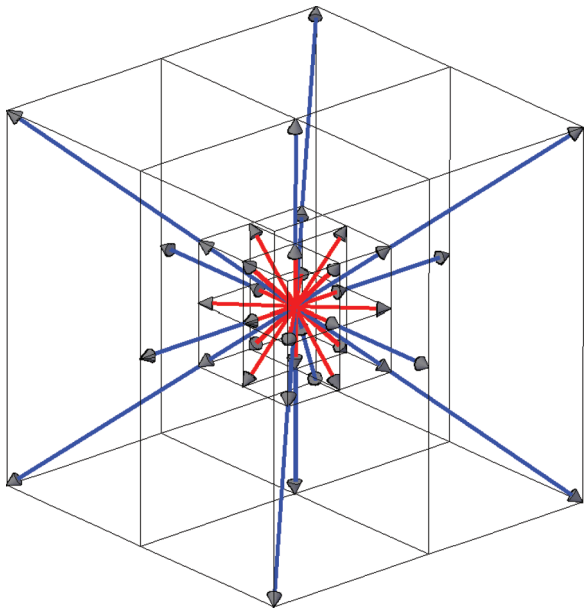

FIG. 1. (Color online) Fourth-order isotropic 19-speed lattice (red arrows) and eighth-order isotropic 41-speed lattice (red and blue arrows).

The relevant hydrodynamic macroscopic moments, i.e., density, linear momentum, and momentum flux tensor, are given by linear weighted sums, namely, $\rho(\vec{x},t)=\sum_i f_i(\vec{x},t)$, $\rho\vec{u}(\vec{x},t)=\sum_i f_i(\vec{x},t)\vec{c}_i$, $\Pi(\vec{x},t)=\sum_i f_i(\vec{x},t)\mathbf{Q}_i$, where $\mathbf{Q}_i = \vec{c}_i\vec{c}_i - c_s^2\mathbf{I}$, $\mathbf{I}$ being the identity matrix.

In this work, we shall use two classes of lattices, the D3Q19 and D3Q41 lattices, providing fourth- and eighth-order isotropy in three dimensions, respectively (see Fig. 1). The standard notation DnQm for m discrete velocities in n spatial dimensions is used throughout. While low-order lattices allow one to correctly recover kinetic moments only up to second order, the eighth-order ones provide sufficient isotropy to retrieve moments up to order four.

The regularized LB reads as follows:

$$f_i(x_i+c_i\Delta t,t+\Delta t) = \mathcal{R}f_i'(x,t) \equiv h_i^{\rm eq} - \frac{\Delta t}{\tau}h_i^{\rm neq}, \quad (4)$$

where h_i is the hydrodynamic component of the full distribution f_i (see Refs. [19,21,27,28]) and $\mathcal{R}$ stands for the regularization operator. From the above, it is appreciated that the postcollision distribution of a fourth-order isotropic lattice is defined only in terms of the relevant hydrodynamic modes, namely, the conserved and the transport ones (ρ, $\rho\vec{u}$, and Π). Also to be noted is that, for eighth-order lattices, the hydrodynamic component also includes third-order moments, namely, $\mathbf{Q}(\vec{x},t)=\sum_i f_i^{\rm eq}(\vec{x},t)\mathbf{Q}_i\vec{c}_i$.

The physical meaning of the regularization is quite transparent: It filters out the nonhydrodynamic moments from the postcollision distribution function, so as to minimize their unphysical effect on the macroscopic behavior of the flow. Indeed, the aim of employing HOLs is not to include nonhydrodynamic moments (ghosts), but the transport modes, namely, nonconserved ones higher than second order, which lie beyond the Navier-Stokes description but still carry a macroscopic meaning.

As we shall see, this is crucial to recover the correct behavior in the high Knudsen regime. As per kinetic boundary conditions, we have employed the diffuse-scattering formulation developed in Ref. [18], namely, a lattice transcription of Maxwell's full accommodation model. In this model, molecules impinging on the wall fully accommodate with the solid ones, and consequently they are reemitted into the fluid along a random direction and with a magnitude drawn from a local Maxwellian at the local wall temperature [29].

A. Extended lattice Boltzmann versus Grad's extended hydrodynamics

It is well known that, back in the 1960's, Grad [23] proposed an elegant procedure, generalized hydrodynamics, to solve the Boltzmann equation via expansion onto suitable sets of basis functions (Hermitian polynomials for the case of Cartesian geometries). This expansion leads to an open-ended hierarchy of first-order nonlinear partial differential equations for the kinetic moments associated with the projection of the Boltzmann distribution upon the chosen basis function. In order to close the hierarchy, Grad proposed to truncate it to the third-order level, i.e., including density, current, momentum flux, and energy flux, for a total of 13 in three spatial dimensions. Despite its elegance, Grad's procedure has met with limited success in practical applications, mainly because the 13-moment truncation no longer guarantees positivity of the distribution function and also because it is hard to impose well-defined boundary conditions, especially in wall bounded flows where more moments are needed to describe anisotropic transport. The LB approach is an alternative way of formulating the Grad's program, by using the discrete distributions instead of Grad's kinetic moments as a mathematical representation. The perceived advantage is that, by including a sufficient number of discrete velocities, the LB can capture finite-Knudsen nonequilibrium effects without incurring the numerical difficulties incurred by the Grad's procedure [24]. More specifically, there are several basic differences between extended LB schemes and Grad's 13 moments method. First, extended LB schemes obviously contain many more moments than Grad's 13 moments method. In particular, extended LB schemes account for third-order tensors not included in Grad's analysis, which play a significant role, especially near solid walls. Second, not all extended LB schemes can be recovered via the Gauss-Hermite quadrature; to this purpose, it suffices to note that Gauss-Hermite nodes beyond the first Brillouin cell do not come in integer sequence, hence they do not correspond to the discrete velocities used in extended LB schemes. Third, while in Grad's 13 moments method the boundary conditions are often ill conditioned, extended LB schemes have shown compliance with well-posed boundary conditions [24]. This is because the interaction of the discrete distributions with the wall can be handled through controlled lattice transcriptions of the boundary conditions used in particle methods, typically direct simulation Monte Carlo (DSMC). In this sense, extended LB schemes are well positioned to capture the best of the worlds.

III. FLOW ACROSS FLAT PLATES AT INCREASING KNUDSEN

The capability of extended LB schemes to reproduce the flow across parallel plates across a broad range of Knudsen numbers has been pointed out before [24,27]. From this study, however, it is not clear whether all three ingredients mentioned above are indeed necessary to achieve quantitative agreement with analytical results and direct Monte Carlo simulation of the Boltzmann equation. To clarify this important issue, we have performed a systematic investigation of different combinations of HOL, KBC, and REG features.

The numerical simulations are performed on a 50×50 grid, over several thousand time steps in order to achieve steady-state conditions. The main results are collected in Fig. 2. From this figure, we see that the regularized D3Q41 with kinetic boundary conditions provides excellent agreement with both analytical asymptotics and DSMC data, across all four Knudsen regimes: continuum, slip, transition, and ballistic. On the contrary, D3Q41 (no regularization) with kinetic boundary conditions overestimates the flow approximately above $\mathrm{Kn} \sim 0.1$, where, for the flow across flat plates, the Kn is defined as

$$\mathrm{Kn} = \nu/(hc_s), \tag{5}$$

where h is the height of the channel.

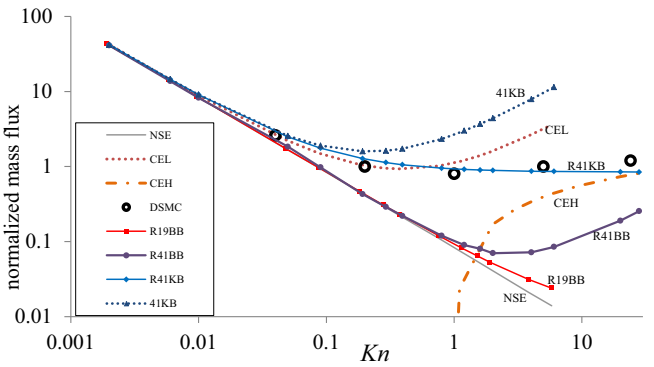

FIG. 2. (Color online) Normalized mass flux across two parallel plane plates as a function of the Knudsen number. Legend: Navier-Stokes solution $1/(12\,\mathrm{Kn})$ (NSE) (solid line), Cercignani solution in the low-Kn slip flow regime [29] (CEL) (dotted line), Cercignani solution in the high-Kn transition and ballistic regimes (CEH) (dashed-dotted line), direct simulation Monte Carlo (DSMC) (circles), regularized D3Q19 LB with bounce-back boundary conditions (R19BB) (solid line with squares), regularized D3Q41 LB with kinetic boundary conditions (R41KB) (solid line with diamonds), regularized D3Q41 LB with bounce-back boundary conditions (R41BB) (solid line with circles), and D3Q41 LB with kinetic boundary conditions (41KB) (dotted line with triangles). Results with regularized D3Q41 LB with the kinetic boundary conditions are omitted because on the scale of the figure they overlap with R19KB. Likewise, D3Q19 LB with kinetic boundary conditions is not shown because it overlaps with the 41KB. The main message here is that higher-order lattices, regularization, and kinetic boundary conditions are required, in order to retrieve the correct behavior of the flow between two plates across all the Knudsen's regimes.

This suggests that the regularization corrects the well-known tendency of the LB lattices to overemphasize the role of the streaming directions which never hit the wall in the collisionless limit ("runaway directions"), thereby leading to an artificial excess of mass flow [12]. Clearly, this anomaly is particularly acute in the flat plate geometry, a point to which we shall return shortly. From the same figure we see that D3Q41R with bounce-back underestimates the flow already at Kn > 0.05, indicating that the excessive slowdown at solid walls caused by the bounce-back conditions is not healed by regularization. Taken all together, the figure shows that both regularization and kinetic boundary conditions are required to retrieve the correct nonequilibrium behavior across all values of the Knudsen numbers. More importantly, it also shows why this is so: Regularization mitigates the "runaway pathology," but cannot cure the excessive loss of momentum to the walls caused by bounce-back boundary conditions.

IV. THREE-DIMENSIONAL FLOW THROUGH REGULAR ARRAYS OF SPHERES

We have noted before that the "runaway pathology" is particularly emphasized by the flat plate geometry. One may wonder whether more complex geometries, such as those encountered in many practical applications, suffer the same pathology. A similar question goes for the overdissipation induced by the bounce-back conditions. Both questions appear relevant to the assessment of the LB approach to geometries of practical interest [30,31]. To shed light on these issues, we have performed systematic simulations of three-dimensional flows through a porous medium formed by an array of simple cubic cells (scc's) of spheres of equal radius, at increasing values of the Knudsen number.

The simulations are performed on a 100^3 grid, with 25 grid points across the radius of the sphere. In lattice units (i.e., $\Delta t = \Delta x = 1$), the Knudsen number is defined as follows,

$$\mathrm{Kn} = \nu/(Dc_s), \tag{6}$$

where D is the sphere diameter. Hence, the Knudsen number can be controlled by varying the viscosity through the relaxation time τ. Due to the geometric properties of the elementary cell, we applied periodic boundary conditions on all six faces of the domain. Both Reynolds and Mach numbers were kept sufficiently low to secure compliance with the incompressible and Darcy limits, respectively.

In Fig. 3 we show the permeability correction factors, defined as the ratio between the apparent permeability (which is a function of Kn) κ and the equivalent liquid permeability or absolute permeability κ_∞, for a broad range of flow regimes. As a reference, we take the analytical correction factors proposed by Klinkenberg [32] and Beskok *et al.* [33], which read, respectively,

$$\kappa = (1 + 4c\,\mathrm{Kn})\kappa_\infty, \tag{7}$$

$$\kappa = [1 + 4\alpha(\mathrm{Kn})\mathrm{Kn}]\left(1 + \frac{4\,\mathrm{Kn}}{1 - b\,\mathrm{Kn}}\right)\kappa_\infty, \tag{8}$$

where c is a constant slightly less than one, α is the rarefaction coefficient, and b is a constant. These two corrections stand, respectively, for the lower and upper bounds for permeability

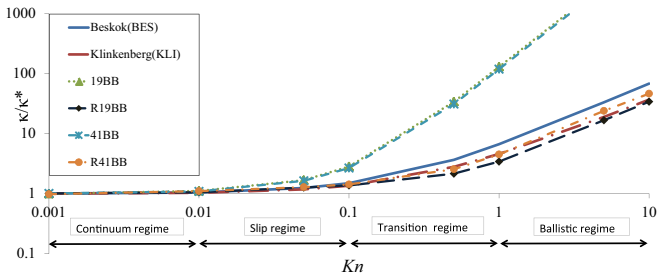

FIG. 3. (Color online) Permeability correction factor as a function of the Knudsen number. The Klinkenberg (KLI) [32] and the Beskok (BES) [33] solutions are reported in solid and dashed-dotted lines, respectively. 19BB (dotted line with triangles), R19BB (dashed line with diamonds), 41BB (dashed line with crosses), and R41BB (dashed-dotted line with circles). It is evident that the nonregularized models can predict accurately the correction factor only within the continuum regime, while they deviate from the analytical solutions already in the slip regime. On the other hand, the R41BB provides correction factors in good agreement with the Klinkenberg solution across the continuum, slip, and transition regimes. When entering the ballistic region, the R41BB begins to overestimate the Klinkenberg discharge while keeping on predicting values of permeability between the Beskok and the Klinkenberg solutions. Here, 19BB stands for the D3Q19 LB with bounce-back boundary conditions, while the other labels are the same as in Fig. 2.

in porous media. Figure 3 carries the central message of this section. First, the D3Q19 and D3Q41 with bounce-back boundary conditions agree with the analytical solutions only in the regime Kn < 0.01. At higher Knudsen's, say, between $0.01 <$ Kn < 0.03, they slightly overestimate the mass flow. For D3Q19 this is no surprise, but the fact that D3Q41 shows the same behavior reveals that higher-order lattices are still exposed to the "runaway" effects. On the other hand, the excessive slowdown due to bounce back is probably still weak in this region of Knudsen numbers, since molecular collisions in the bulk are much more frequent than fluid-solid collisions at the wall. At higher Knudsen's, both models substantially overestimate the permeability, which is also understandable in view of the increasing role of runaway effects. Summarizing, to this point, HOL alone is powerless. Let us now consider the effect of regularization while still sticking to bounce-back conditions. From Fig. 3, it is clearly appreciated that regularization provides a dramatic improvement at all Knudsen numbers, even with the standard 19-speed lattice. Indeed, the mass flow fits both the Klinkenberg and the Beskok solutions in the slip regime and in the first half of the transition zone (up to Kn $\simeq 0.3$). At higher Knudsen numbers, D3Q19R slightly underestimates the Klinkenberg solution, but still keeps providing reasonable results both in the transition and in the free-molecular regimes. This shows that, even without higher-order lattices, the artifacts due to runaway directions and bounce-back boundary conditions are substantially suppressed by the regularization procedure. The use of higher-order lattices further improves the situation. Indeed, upon inspecting Fig. 3, a remarkably good agreement with the Klinkenberg solution across all four Knudsen regimes is appreciated. When entering the ballistic region, Kn > 1, the D3Q41R starts to overestimate the Klinkenberg discharge,

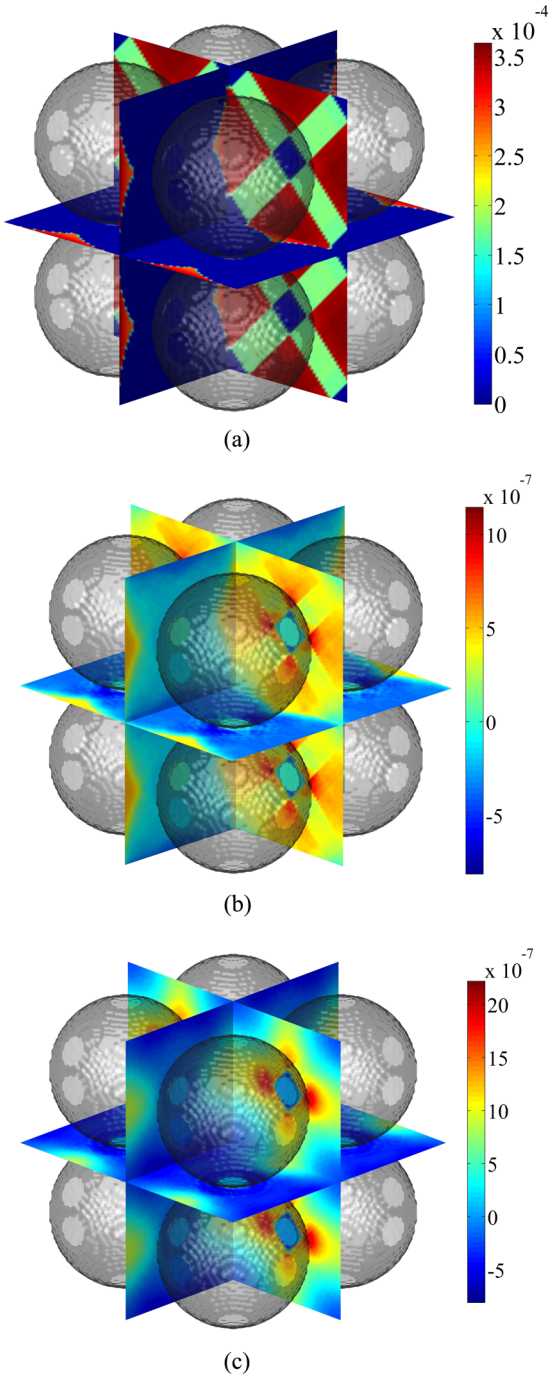

FIG. 4. (Color online) Q_{xxz} field on midplanes of the porous media at Kn = 5. (a) The D3Q19 exposes in full the lattice structure, which betrays its lack of isotropy towards third-order moments. As expected, D3Q19R is powerless against this structural deficiency, as shown in (b). (c) The D3Q41R appears both isotropic and noise free.

but still remains between the Beskok and the Klinkenberg solutions. This is a remarkable result, especially in view of the fact that we are using a very simple single-time relaxation model with bounce-back boundary conditions. To gain further insight into this welcome behavior, we have monitored the spatial distribution of a number of representative *third*-order kinetic moments, i.e., the ones carrying the generalized hydrodynamic information. In Fig. 4, we show the Q_{xzz} field at Kn = 5, i.e., the flux along the mainstream direction x of the partial kinetic energy along the z direction, on three midplanes. These are prototypical moments *not* included in the original Grad's formulation. From these figures, we see that D3Q19 exposes in full the lattice structure, which betrays a lack of isotropy of the third-order moments. As shown, D3Q19R is powerless against this structural deficiency. Finally, D3Q41R appears both isotropic and noise free. Although qualitatively consistent with the picture of the extended LB strategy presented in this work, these results still need quantitative comparison with direct simulation of the Boltzmann equation.

V. SUMMARY AND OUTLOOK

Summarizing, we have shown that for parallel plate flows only, all three ingredients of the extended LB method, namely, a standard LB enriched with regularization step, high-order lattices, and kinetic boundary conditions, are necessary to quantitatively accomplish Grad's extended hydrodynamics program. We have also shown that the mass flow across a regular array of spheres can be quantitatively captured across the full range of Knudsen numbers, by just regularizing the standard LB scheme, without using kinetic boundary conditions.

A quantitative statement on the internal structure of the flow, on the other hand, must await for a systematic comparison with a direct solution of the Boltzmann equation for the geometry setups discussed in this paper. Before closing, we hasten to add that our results by no means imply that the extended LB schemes presented in this work can capture the physics contained in the Boltzmann equation in full generality. What they imply is simply that the gap between the two can be significantly narrowed for the specific cases explored in this work. This opens different perspectives for the simulation of strong nonequilibrium flows, either with extended LB standalone schemes or in connection with DSMC for advanced multiscale applications.

ACKNOWLEDGMENTS

The research has been supported by the Italian national project "Hydroelectric energy by osmosis in coastal areas," PRIN 2010-2011. This work was also supported by the Integrated Mesoscale Architectures for Sustainable Catalysis (IMASC) Energy Frontier Research Center (EFRC) of the Department of Energy, Basic Energy Sciences, Award No. DE-SC0012573.

[1] R. B. Schoch, J. Han, and P. Renaud, Rev. Mod. Phys. **80**, 839 (2008).
[2] J. C. Eijkel and A. Van Den Berg, Microfluid. Nanofluid. **1**, 249 (2005).
[3] G. Karniadakis, A. Beskok, and N. Aluru, *Microflows and Nanoflows: Fundamentals and Simulation*, Vol. 29 (Springer, Berlin, 2006).
[4] S. Succi, Phys. Rev. Lett. **89**, 064502 (2002).

[5] J. Zhang, Microfluid. Nanofluid. **10**, 1 (2011).
[6] S. Succi, G. Smith, and E. Kaxiras, J. Stat. Phys. **107**, 343 (2002).
[7] S. Ansumali, I. V. Karlin, S. Arcidiacono, A. Abbas, and N. I. Prasianakis, Phys. Rev. Lett. **98**, 124502 (2007).
[8] S. Ansumali, I. Karlin, C. E. Frouzakis, and K. Boulouchos, Physica A (Amsterdam) **359**, 289 (2006).
[9] A. Cali, S. Succi, A. Cancelliere, R. Benzi, and M. Gramignani, Phys. Rev. A **45**, 5771 (1992).
[10] S. Succi, Europhys. Lett. **109**, 50001 (2015).
[11] G. H. Tang, W. Q. Tao, and Y. L. He, Phys. Rev. E **72**, 056301 (2005).
[12] F. Toschi and S. Succi, Europhys. Lett. **69**, 549 (2005).
[13] S. H. Kim, H. Pitsch, and I. D. Boyd, J. Comput. Phys. **227**, 8655 (2008).
[14] X. Shan, X.-F. Yuan, and H. Chen, J. Fluid Mech. **550**, 413 (2006).
[15] S. S. Chikatamarla and I. V. Karlin, Phys. Rev. E **79**, 046701 (2009).
[16] R. Machado, Front. Phys. **9**, 490 (2014).
[17] A. Montessori, G. Falcucci, M. La Rocca, S. Ansumali, and S. Succi, J. Stat. Phys., doi: 10.1007/s10955-015-1318-6.
[18] S. Ansumali and I. V. Karlin, Phys. Rev. E **66**, 026311 (2002).
[19] R. Zhang, X. Shan, and H. Chen, Phys. Rev. E **74**, 046703 (2006).
[20] J. Latt and B. Chopard, Math. Comput. Simul. **72**, 165 (2006).
[21] A. Montessori, G. Falcucci, P. Prestininzi, M. La Rocca, and S. Succi, Phys. Rev. E **89**, 053317 (2014).
[22] A. Montessori, M. La Rocca, G. Falcucci, and S. Succi, Int. J. Mod. Phys. C **25**, 1441003 (2014).
[23] H. Grad, Commun. Pure Appl. Math. **2**, 331 (1949).
[24] S. S. Chikatamarla, S. Ansumali, and I. V. Karlin, Europhys. Lett. **74**, 215 (2006).
[25] R. Benzi, S. Succi, and M. Vergassola, Phys. Rep. **222**, 145 (1992).
[26] A. Kupershtokh, D. Medvedev, and D. Karpov, Comput. Math. Appl. **58**, 965 (2009).
[27] X.-D. Niu, S.-A. Hyodo, T. Munekata, and K. Suga, Phys. Rev. E **76**, 036711 (2007).
[28] H. Chen, R. Zhang, I. Staroselsky, and M. Jhon, Physica A (Amsterdam) **362**, 125 (2006).
[29] C. Cercignani, *The Boltzmann Equation and Its Applications* (Springer, Berlin, 1988).
[30] P. Prestininzi, A. Montessori, M. La Rocca, and S. Succi, Int. J. Mod. Phys. C, doi: 10.1142/S0129183116500376
[31] J. Meng, X.-J. Gu, and D. R. Emerson, arXiv:1508.02209.
[32] L. Klinkenberg *et al.*, in *Drilling and Production Practice* (American Petroleum Institute, Washington, D.C., 1941).
[33] A. Beskok and G. E. Karniadakis, Microscale Thermophys. Eng. **3**, 43 (1999).